



***In silico* Study of Adenylyl Cyclase Type 2 Inhibitors**

Syeda Zahra Abbas¹, Ayesha Altaf¹, Syed Kashif Ali, Syeda Tahira Qousain Naqvi^{1*}, Umair Ilyas², Muhammad Imran Qadir¹, Syed Aun Muhammad^{1*}

¹Institute of Molecular Biology and Biotechnology, Bahauddin Zakariya University Multan, Pakistan

²Riphah Institute of Pharmaceutical Sciences, RIU Islamabad, Pakistan

Syeda Zahra Abbas, Email: zahra_abbas110@hotmail.com

Ayesha Altaf, Email: ayshabhatti21@gmail.com

Syed Kashif Ali, Email: kashif93252@gmail.com

Syeda Tahira Qousain Naqvi, Email: tahira22oct@yahoo.com (Corresponding Author)

Muhammad Imran Qadir, Email: mrimranqadir@hotmail.com

Umair Ilyas, Email: umair.ilyas@riphah.edu.pk

Syed Aun Muhammad, Email: aunmuhammad78@yahoo.com (Co-Corresponding Author)

Abstract

Adenylyl cyclase type 2 (ADCY2) is a membrane-associated enzyme responsible for tumor metastasis and progression of many cancer types and therefore can be considered as a therapeutic target. The synthesis of the molecules under investigation in this study, including 4-amino-5-(2-hydroxyphenyl)-1,2,4-triazole-3-thione (UA1) and 4-(2-hydroxybenzalidine) amine-5-(2-hydroxy) phenyl-1,2,4-triazole-3-thiol (UA2), was done at 160°C through fusion technique, are effective inhibitor of ADCY2 enzyme. The UA1 and UA2 were structurally characterized using FTIR and NMR. We analyzed the binding interaction of these compounds with ADCY2 by molecular docking. The docked energy calculated for UA1 and UA2: -4.4328 and -5.2686 kcal/mol respectively. This study would help to design new anti-cancerous agents to improve the therapeutic options against cancer.

KEYWORDS: ADCY2, lead compounds, triazole derivatives, anticancer molecules, structural characterization, computational analysis

Introduction

Cancer refers to abnormal cellular proliferation that leads to epigenetic and cellular level changes. The expression of cancer phenotype requires multiple genetic changes which include point mutation, deletion, and translocation (Shillitoe *et al.*, 2000; Bird, 2002; Baylin and Jones, 2011). Inactivation of tumor suppressor genes that have a protective role against malignant phenotype can result in carcinogenesis. ADCY2 is a member of the class-B in adenylyl cyclase's family, located on chromosome-5, and is considered a candidate gene for cancer (Li *et al.*, 2014). Aberrant DNA methylation of ADCY2 causes colorectal and prostate cancer. It has been observed that the level of ADCY2 is up-regulated in various cancer types and therefore, inhibition of ADCY2 leads to therapeutic response and can be considered as a potential drug target for the treatment of cancer (Herman *et al.*, 1994; Herman *et al.*, 1998; Catto *et al.*, 2005; Zheng *et al.*, 2004). This gene is insensitive to Ca²⁺ and in the case of colorectal cancer hypermethylation-low, gene expression is observed in calcium signaling pathways (Li *et al.*, 2014). Short-term anticancer effects can be induced by DNA hypomethylation but it may speed up tumor progression in cancer cells surviving demethylation chemotherapy, therefore some chemical inhibitor is required to counteract the activity (Ehrlich, 2002).

The development of chemotherapeutic drugs against cancer treatment is a slow process, because of high mutation rates, uncharacterized genetic basis, and expensive techniques. Therefore, new drug development strategies are required to identify new therapeutic drugs for the treatment of cancer, through epigenetic investigations. The *in silico* investigation is a more economic and efficient technique to design targeted-structural drugs, rather than conventional drug discovery through ligand (Muhammad *et al.*, 2014; Mdluli and Spigelman, 2006). Such techniques have become the necessary component for drug discovery and drug-development investigations (Bajorath, 2002). ADCY2 inhibitors as triazole derivatives are projected through optimized binding affinity and minimum binding energy. Triazoles have been used in the development of novel ligand which has attained much importance of pharmaceutical industry due to its biological as well as therapeutic (anti-

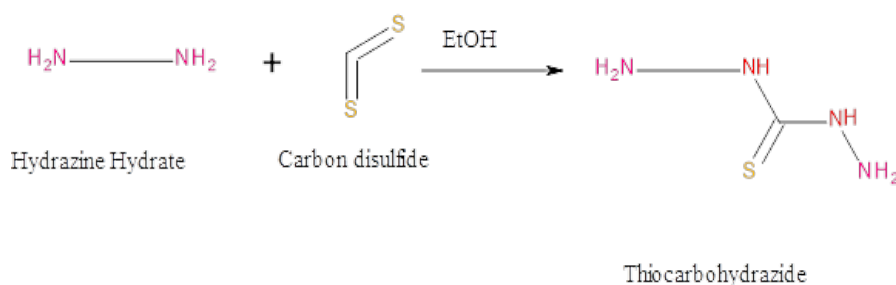
microbial or anti-cancerous) activities (Bekircan and Gümrükçüoğlu, 2005). This analysis is designed to investigate the anti-cancerous activity of the synthesized triazole derivatives against ADCY2.

Materials and Methods

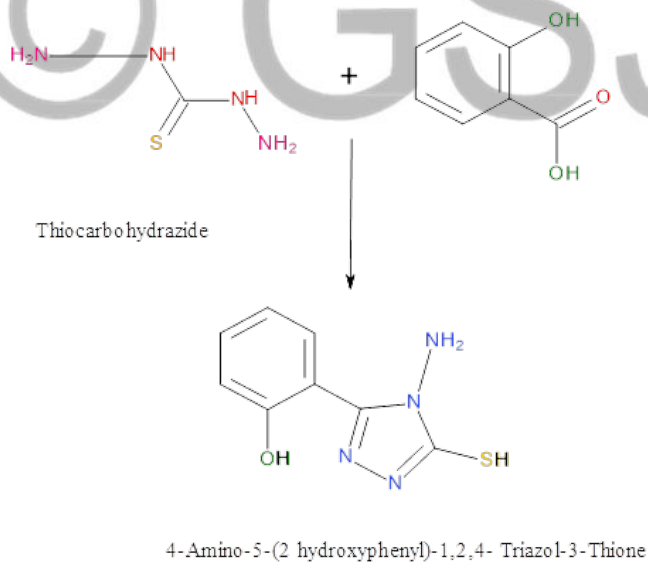
Ligand synthesis

UA1: 4-amino-5-(2-hydroxyphenyl)-1, 2,4-triazole-3-Thione and UA2: 4-(2-hydroxybenzimidine) amine-5-(2-hydroxy) phenyl-1,2,4-triazole-3-thiol, synthesis was carried out as reported in (Muhammad *et al.*, 2014).

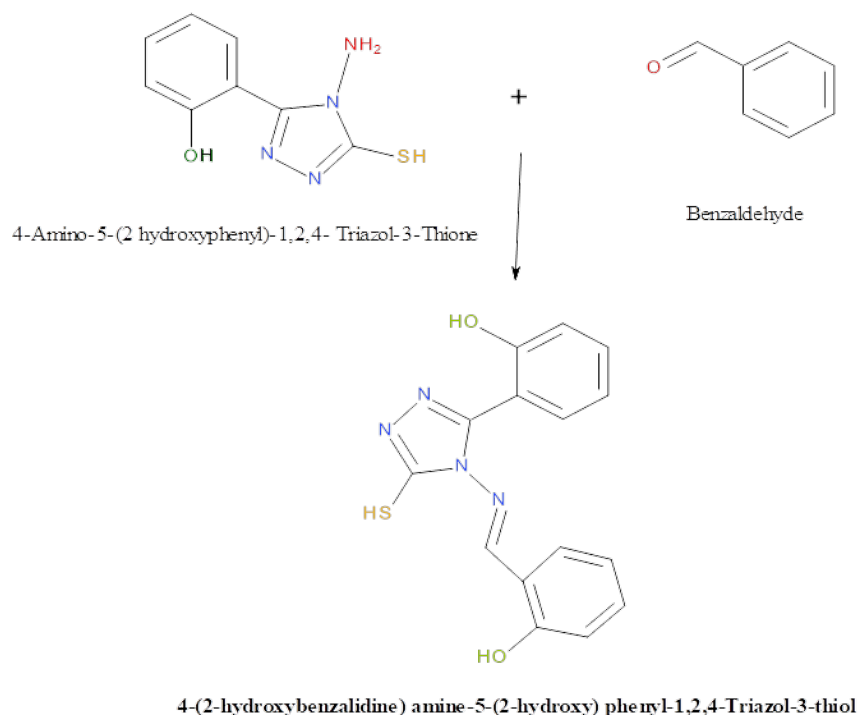
Step 1. Thiocarbohydrazide was synthesized by heating hydrazine hydrate (30ml) and carbon disulfide (15ml) at a reflux condenser for about 4h in the presence of ethanol (150ml).



Step 2. UA1 was synthesized by fusing salicylic acid and thiocarbohydrazide in equimolar quantities, i.e., 0.1 mol, respectively. The mixture is continuously stirred at 160°C for 2h in an oil bath followed by thin-layer chromatography (TLC). The mixture is cooled, filtered, and recrystallized from 70% ethanol after the reaction is completed.



Step 3. UA2 was synthesized by dissolving 1 gram of UA1 in ethanol and an equimolar quantity of benzaldehyde was added at constant stirring for approximately 4 hours, and TLC determines the completion of the reaction.



Structural characterization

Fourier-transform infrared spectroscopy (FTIR) was used for the characterization of the structure and physical properties of these compounds. The interferogram results were recorded in the range of 3600–650 cm^{-1} wavelength. Preparation of NMR samples was done by taking 15mg in 0.5ml ddH₂O and a Bruker spectrometer of 300MHz equipped with a 5mm probe head was used for NMR spectral ¹H analysis.

Drug likeness and pharmacokinetics

The drug-likeness and Pharmacokinetic properties of these compounds were predicted using the Swiss ADME tool (Daina *et al.*, 2017). According to these properties, the molecule must attain certain physicochemical, drug-likeness, and kinetics parameters with minimum to zero violations. Generally, in a good drug, the molecules would be water-soluble, having lead likeness features, and fulfill some criteria including hydrogen bond donor's <5 (OH and NH groups), hydrogen bond acceptors <10 (N and O atoms), molecular weight <500 Da, and log P coefficient (C log P) less than 5 (Muhammad *et al.*, 2014).

Preparation of Ligand Molecules and Accession of Target Protein

The chemical structures of both ligand UA1 and UA2 were prepared through Accelrys Draw. During this analysis, the Mol SDF format was used for both ligands. The 3D structure of ADCY2 was modeled using the Pyre tool (Kelley *et al.*, 2015) and the quality of the model was assessed.

The active binding site and molecular docking analysis

The active site for targeted protein was analyzed through MOE (Molecular operating environment). It defines the coordinates with ligand for the active site of the original target protein. The structural complexes in ADCY2 with triazole derivatives were determined by computational ligand-target docking using the software MOE. These triazole derivatives and

target proteins were assigned grid points through their interacting energies. The interaction energy of ligand and protein was analyzed at every step.

Results

Synthesis of lead molecules

The ADCY2 inhibitors (UA1 and UA2) were synthesized at melting temperatures 120⁰C and 170⁰C, correspondingly. The solubility of both of these compounds in ethanol with R_f-value of 0.16 and 0.12, respectively was observed (Table 1).

Spectral analysis

The functional groups of UA1 and UA2, peak values were confirmed by FITR. UA1 showed a spectral peak at 3137 cm⁻¹ for OH and UA2 at 3061-3100 cm⁻¹. The observed characteristic stretching vibrations were observed at 1591 and 1599 cm⁻¹ for UA1 and UA2 respectively. These compounds are formed by cyclo-condensation confirmed by the absence of absorption band spectra of N, H, and O (Table 2). As ¹H NMR spectral signals predicted about aliphatic and aromatic group molecules. For UA1: [H NMR (DMSO, 300 MHz, 5 ppm): 7.25–7.37 (m, 4H, Ar-H), 5.37 (s, 2H, NH₂), 10.3 (bS, 1H, OH), 13.9 (S, 1H, SH)] and for UA2: [7.28–7.43 (m, 8H, Ar-H), 9.1 (S, 1H, CH), 10.5 (bS, 2H, OH), 13.8 (9S, 1H, SH)].

Predicting pharmacokinetics and drug-likeness properties

The radar graph exhibited the summary of UA1 and UA2 ligands indicating most of the features are within the highlighted region. The physicochemical properties showed the intrinsic properties of these molecules presenting lead-like characteristics. The pharmacokinetics parameters showed that our ligands do not inhibit and affect the metabolic enzymes especially cytochrome p-450 indicating non-interference in metabolic activities. Our ligands passed the drug-likeness rules including Lipinski, Ghose, Veber with zero violation. These ligands showed a significant bioavailability score (0.55). For UA1: molecular weight: 312.354, log p-value is 3.397, and the number of violation 0.0 and for UA2 the value of partition coefficient log P: 1.407, the molecular weight is 208.46 along with the number of violations 0.0 were shown (Figure 1).

Protein model quality analysis

Our protein model quality showed that 40% modeled through 100% confidence and 50% can be modeled at >90% confidence with multiple templates. The Ramachandran plot analysis revealed, ≥90% of amino acid residues for the predicted model are in the favored region, only 2% or less were present in the disallowed region. This analysis also indicates the lower energy conformations regarding psi and phi, though the target protein backbone conformation is shown in graphical representation (Figure 2).

Analysis of active site and molecular docking

The active site is analyzed on the surface of ADCY2 indicating the probable binding pocket for ligands interaction (Figure 3). Ligand UA1 showed binding with LYS989, PHE978, GLY982, VAL981, ALA985, ASN1077, LEU1084, SER1083, ARG1082, and LYS1039 amino acid residues of ADCY2 target while UA2 showed interactions with LYS989, SER1081, VAL981, PHE978, PHE1075, ASN1077, ARG1082, ASP1038, LYS1039, LYS996, SER1083 amino acid residues as shown in (Figure 4). Therefore, the final dock

energy calculated for UA1: -4.2328kcal/mol and for UA2: -5.2686kcal/mol. Docking results and their binding energy information was given (Table 3 and 4).

Discussion

In this study, we performed the docking analysis of the triazoles derivatives (Muhammad *et al.*, 2014) with human ADCY2. In previous studies, it was revealed that expression of ADCY2 is dysregulated in many cancer types including colorectal, urinary bladder, oral, small cell lung, and breast carcinomas (Zheng *et al.*, 2004; Liu *et al.*, 2017; Severino *et al.*, 2008; Frye *et al.*, 2010; Taniwaki *et al.*, 2006), that permits this enzyme to act as a therapeutic target. Due to the lack of metastatic-stage treatments and proliferation of the ADCY2, the study adds significant advances, by the synthesizing of chemotherapeutic agents which emphasize new treatment which will reduce or block the activity of ADCY2. The synthesis of anti-cancerous amino acid, triazoles, was done through the reaction of salicylic acid and thiocarbohydrazide at 160°C, which leads to the formation of UA1 (4-amino-5-(2-hydroxyphenyl)-1,2,4-triazole-3-thione) and UA2 (4-(2-hydroxybenzalidine) amine-5-(2-hydroxy) phenyl-1,2,4-triazole-3-thiol).

The structural properties of these compounds made them an important active compound, and are known to possess antimicrobial and anti-cancerous activity. Therefore, these triazole compounds are known for their solubility in ethanol through the relevant flow of 0.12 and 0.16. Other properties including molecular weight, partition coefficient, and other pharmacokinetic properties passed the RO5 (rule of 5) with zero violation (Zaid *et al.*, 2010). The peak values were observed from the functional group of the triazole molecules through the obtained spectral data. There were no absorption bands for N-H and C=O that proved their formation by cyclo condensation. The FTIR peaks showed distinctive absorption bands for >C=N, or C-N, whose triazole ring was observed at 1562–1598cm⁻¹ and 1313–1365cm⁻¹ respectively (Prakash *et al.*, 2004). Correspondingly, the data spectral signals from ¹H NMR showed aliphatic and aromatic group presence. Similarly, S-H presence, C=S absence, and absorption of N-H proposed thiol form existence of triazole ring in the compounds (Prakash *et al.*, 2004; Sztanke *et al.*, 2006).

The association of ADCY2 in cancer development and proliferation inhibition can be an effective way of treating cancer (Frye *et al.*, 2010; Taniwaki *et al.*, 2006), using these heterocyclic triazoles. The *in-silico* ligand-binding affinity for target gene and ligands, confirmed the effective binding energies between ligand and target protein, -4.4328 and -5.2686 kcal/mol for UA1 and UA2, respectively. UA2 had with greater binding affinity with the target gene rather than UA1 and both triazole derivative ligands can be showed anti-cancerous activity.

Conclusion

The *in-silico* screening and docking analysis of triazole molecules as drug ligands is a remarkable approach that helps to understand protein-ligand affinity. The inhibition of adenylyl cyclase type-2 enzyme by triazole derivatives can be considered as an effective anticancer therapeutic option. The energy values of the triazole molecule and target protein complexes are stabilized by the intermolecular interaction that can be investigated for further experimental use.

References

- E.J. Shillitoe, M. May, V. Patel, C. Lethanakul, J.F. Ensley, R.L. Strausberg and J.S. Gutkind, "Genome-wide analysis of oral cancer—early results from the Cancer Genome Anatomy Project," *Oral Oncol.* Vol. 36 no. 1 pp. 8-16, 2000.
- A. Bird, "DNA methylation patterns and epigenetic memory," *Genes Dev.* Vol. 16 no. pp. 6-12, 2002.
- S.B. Baylin and P.A. Jones, "A decade of exploring the cancer epigenome—biological and translational implications," *Nat. Rev. Cancer.* Vol. 11 no. pp. 726–734, 2011.
- Y.X. Li, H.G. Jin, C.G. Yan, C.Y. Ren, C.J. Jiang, C.D. Jin, K.S. Seo and X. Jin, "Molecular cloning, sequence identification, and gene expression analysis of bovine ADCY2 gene," *Mol. Biol. Rep.* Vol. 41 no. 6 pp. 3561-3568, 2014.
- J.G. Herman, F. Latif, Y. Weng, M.I. Lerman, B. Zbar, S. Liu, D. Samid, D.S. Duan, J.R. Gnarr and W.M. Linehan, "Silencing of the VHL tumor-suppressor gene by DNA methylation in renal carcinoma," *Proc. Natl. Acad. Sci.* Vol. 91 no. 21 pp. 9700-9704, 1994.
- J.G. Herman, A. Umar, K. Polyak, J.R. Graff, N. Ahuja, J.-P.J. Issa, S. Markowitz, J.K.V. Willson, S.R. Hamilton, K.W. Kinzler, M.F. Kane, R.D. Kolodner, B. Vogelstein, T.A. Kunkel and S.B. Baylin, "Incidence and functional consequences of hMLH1 promoter hypermethylation in colorectal carcinoma," *Proc. Natl. Acad. Sci.* Vol. 95 no. 12 pp. 6870-6875, 1998.
- J.W.F. Catto, A.-R. Azzouzi, I. Rehman, K.M. Feeley, S.S. Cross, N. Amira, G. Fromont, M. Sibony, O. Cussenot, M. Meuthand F.C. Hamdy, "Promoter Hypermethylation Is Associated With Tumor Location, Stage, and Subsequent Progression in Transitional Cell Carcinoma," *Int. J. Clin. Oncol.* Vol. 23 no. 13 pp. 2903-2910, 2005.
- M. Zheng, R. Simon, M. Mirlacher, R. Maurer, T. Gasser, T. Forster, P.A. Diener, M.J. Mihatsch, G. Sauter and P. Schraml, "TRIO amplification and abundant mRNA expression is associated with invasive tumor growth and rapid tumor cell proliferation in urinary bladder cancer," *The American journal of pathology* Vol. 165 no. 1 pp. 63-69, 2004.
- M. Ehrlich, "DNA methylation in cancer: too much, but also too little," *Oncogene* Vol. 21 no. pp. 5400, 2002.
- S.A. Muhammad, A. Ali, T. Ismail, R. Zafar, U. Ilyas and J. Ahmad, "In silico study of anti-carcinogenic lysyl oxidase-like 2 inhibitors," *Comput. Biol. Chem.* Vol. 51 no. pp. 71-82, 2014.
- K. Mdluli and M. Spigelman, "Novel targets for tuberculosis drug discovery," *Curr. opin. pharmacol.* Vol. 6 no. 5 pp. 459-467, 2006.
- J. Bajorath, "Integration of virtual and high-throughput screening," *Nat. Rev. Drug. Discov.* Vol. 1 no. pp. 882–894, 2002.
- O. Bekircan and N. Gümrukçüoğlu, "Synthesis of some 3, 5-diphenyl-4H-1, 2, 4-triazole derivatives as antitumor agents," *Indian J. Chem.* Vol. 44B no. pp. 2107-2113, 2005.
- A. Daina, O. Michielin and V. Zoete, "SwissADME: a free web tool to evaluate pharmacokinetics, drug-likeness and medicinal chemistry friendliness of small molecules," *Sci. Rep.* Vol. 7 no. pp. 1-13, 2017.
- L.A. Kelley, S. Mezulis, C.M. Yates, M.N. Wass and M.J.E. Sternberg, "The Pyre2 web portal for protein modeling, prediction and analysis," *Nat. Protoc.* Vol. 10 no. pp. 845-858, 2015.
- J. Liu, H. Li, L. Sun, Z. Wang, C. Xing and Y. Yuan, "Aberrantly methylated-differentially expressed genes and pathways in colorectal cancer," *Cancer Cell Int.* Vol. 17 no. 1 pp. 1-10, 2017.
- P. Severino, A.M. Alvares, P. Michaluart, Jr., O.K. Okamoto, F.D. Nunes, C.A. Moreira-Filho, E.H. Tajara, Head and G. Neck Genome Project, "Global gene expression profiling of oral cavity cancers suggests molecular heterogeneity within anatomic subsites," *BMC Res. Notes* Vol. 1 no. pp. 113-113, 2008.
- M. Frye, I. Dragoni, S.-F. Chin, I. Spiteri, A. Kurowski, E. Provenzano, A. Green, I.O. Ellis, D. Grimmer, A. Teschendorff, C.C. Zouboulis, C. Caldas and F.M. Watt, "Genomic gain of 5p15 leads to over-expression of Misu (NSUN2) in breast cancer," *Cancer Lett.* Vol. 289 no. 1 pp. 71-80, 2010.
- M. Taniwaki, Y. Daigo, N. Ishikawa, A. Takano, T. Tsunoda, W. Yasui, K. Inai, N. Kohno and Y. Nakamura, "Gene expression profiles of small-cell lung cancers: molecular signatures of lung cancer," *Int. J. Oncol.* Vol. 29 no. 3 pp. 567-575, 2006.
- H. Zaid, J. Raiyn, A. Nasser, B. Saad and A. Rayan, "Physicochemical properties of natural based products versus synthetic chemicals," *Open Nutraceuticals J.* Vol. 3 no. pp. 194-202, 2010.

- O. Prakash, V. Bhardwaj, R. Kumar, P. Tyagi and K.R. Aneja, "Organiodine (III) mediated synthesis of 3-aryl/hetaryl-5,7-dimethyl-1,2,4-triazolo[4,3-a]pyrimidines as antibacterial agents," *Eur. J. Med. Chem.* Vol. 39 no. 12 pp. 1073-1077, 2004.
- K. Sztanke, K. Pasternak, A. Sidor-Wójtowicz, J. Truchlińska and K. Józwiak, "Synthesis of imidazoline and imidazo[2,1-c][1,2,4]triazole aryl derivatives containing the methylthio group as possible antibacterial agents," *Bioorg. Med. Chem.* Vol. 14 no. 11 pp. 3635-3642, 2006.

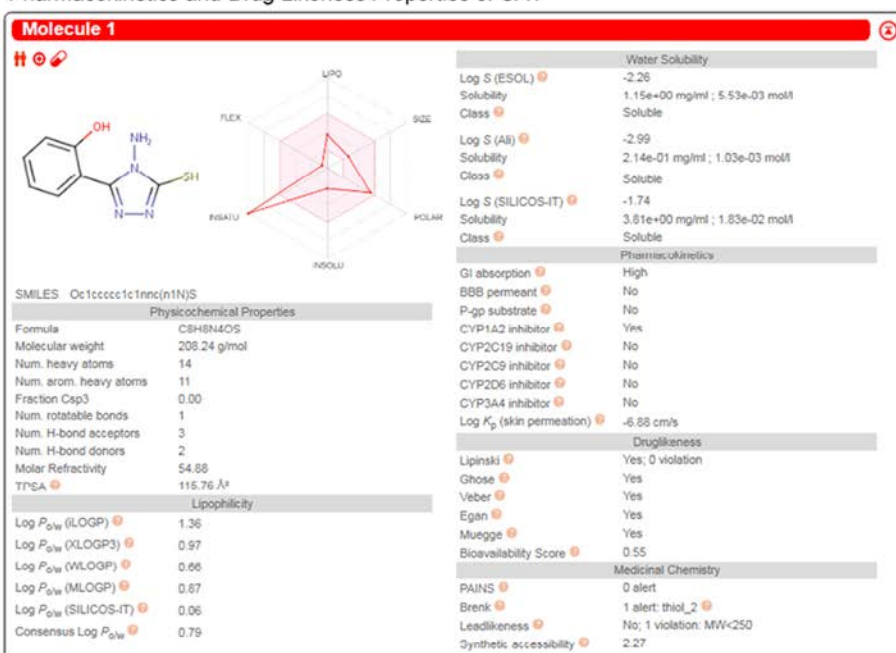
© GSJ

FIGURE LEGENDS

- Figure 1:** Pharmacokinetic properties, drug-likeness, and physicochemical properties of UA1 and UA2 ligands.
- Figure 2:** The conformational and helical structure of adenylyl cyclase type 2 protein model. Ramachandran plot ADCY2 confirmed the quality of the protein model constructed by Drug Discovery Studio version 3.0 indicated that the amino acid residues occur in the “favored region” of the plot. For a good protein model, there must be $\geq 90\%$ amino acid residues in the most “favored region” or $< 2\%$ in the “disallowed region” of the plot.
- Figure 3:** Active binding site of ADCY2 target showed by binding pocket for ligands interaction.
- Figure 4:** Molecular docking and binding interaction of UA1 and UA2 with the target protein.

© GSJ

Pharmacokinetics and Drug Likeness Properties of UA1



Pharmacokinetics and Drug Likeness Properties of UA2

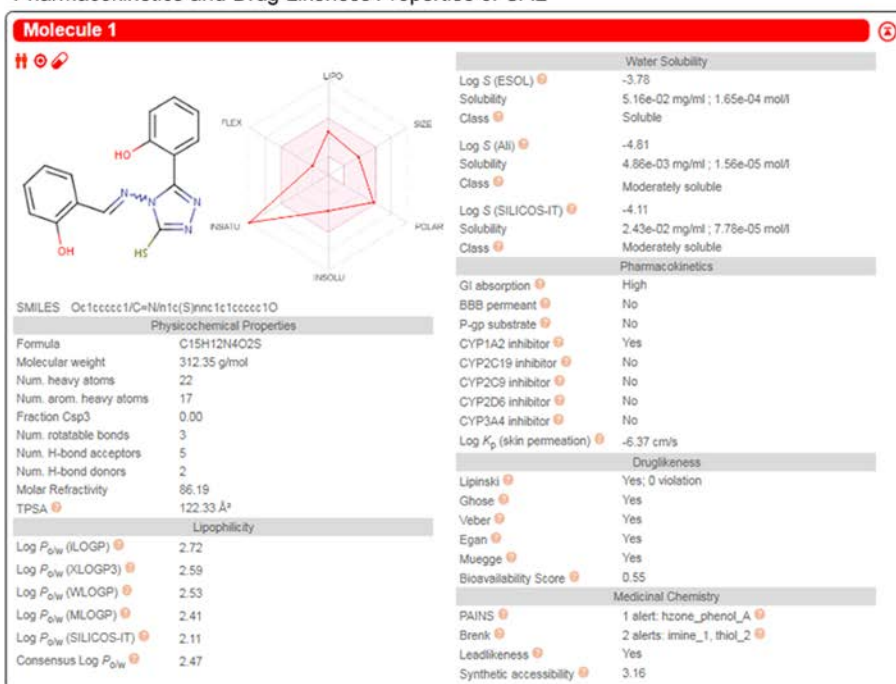


Figure 1: Pharmacokinetic properties, drug-likeness, and physicochemical properties of UA1 and UA2 ligands.

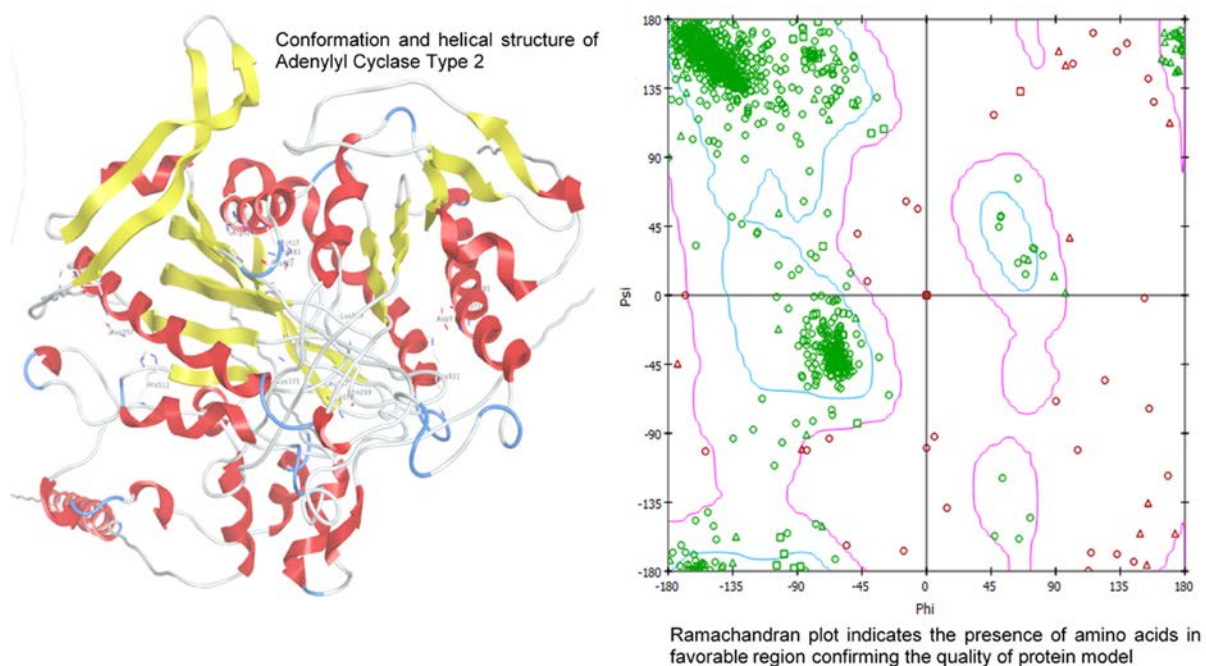


Figure 2: The conformational and helical structure of adenylyl cyclase type 2 protein model. Ramachandran plot ADCY2 confirmed the quality of the protein model constructed by Drug Discovery Studio version 3.0 indicated that the amino acid residues occur in the “favored region” of the plot. For a good protein model, there must be $\geq 90\%$ amino acid residues in the most “favored region” or $< 2\%$ in the “disallowed region” of the plot.

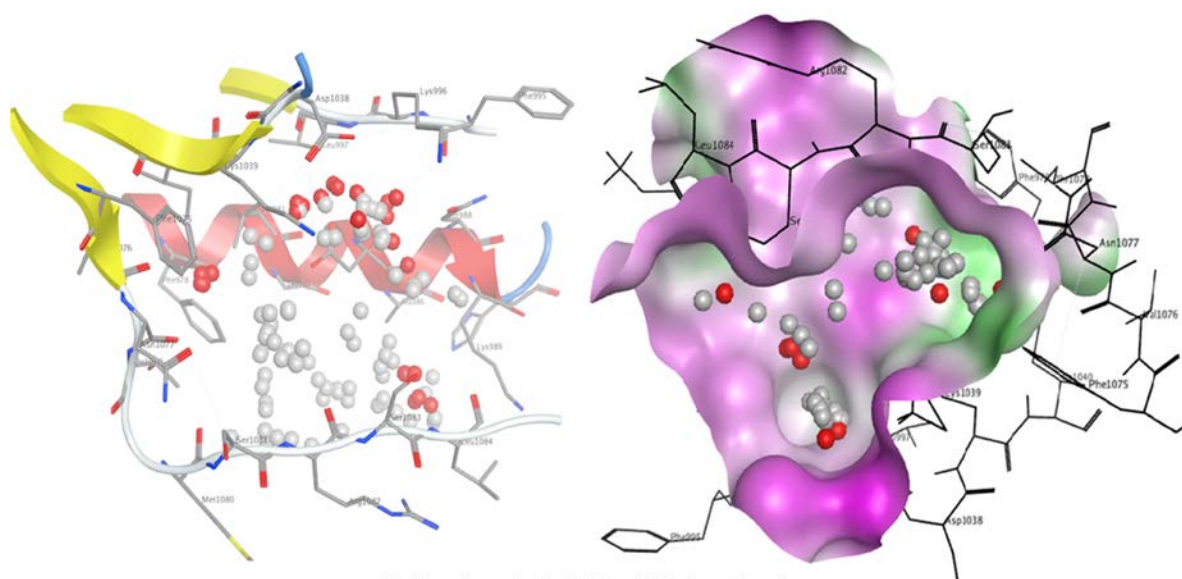


Figure 3: Active binding site of ADCY2 target showed by binding pocket for ligands interaction.

© GSJ

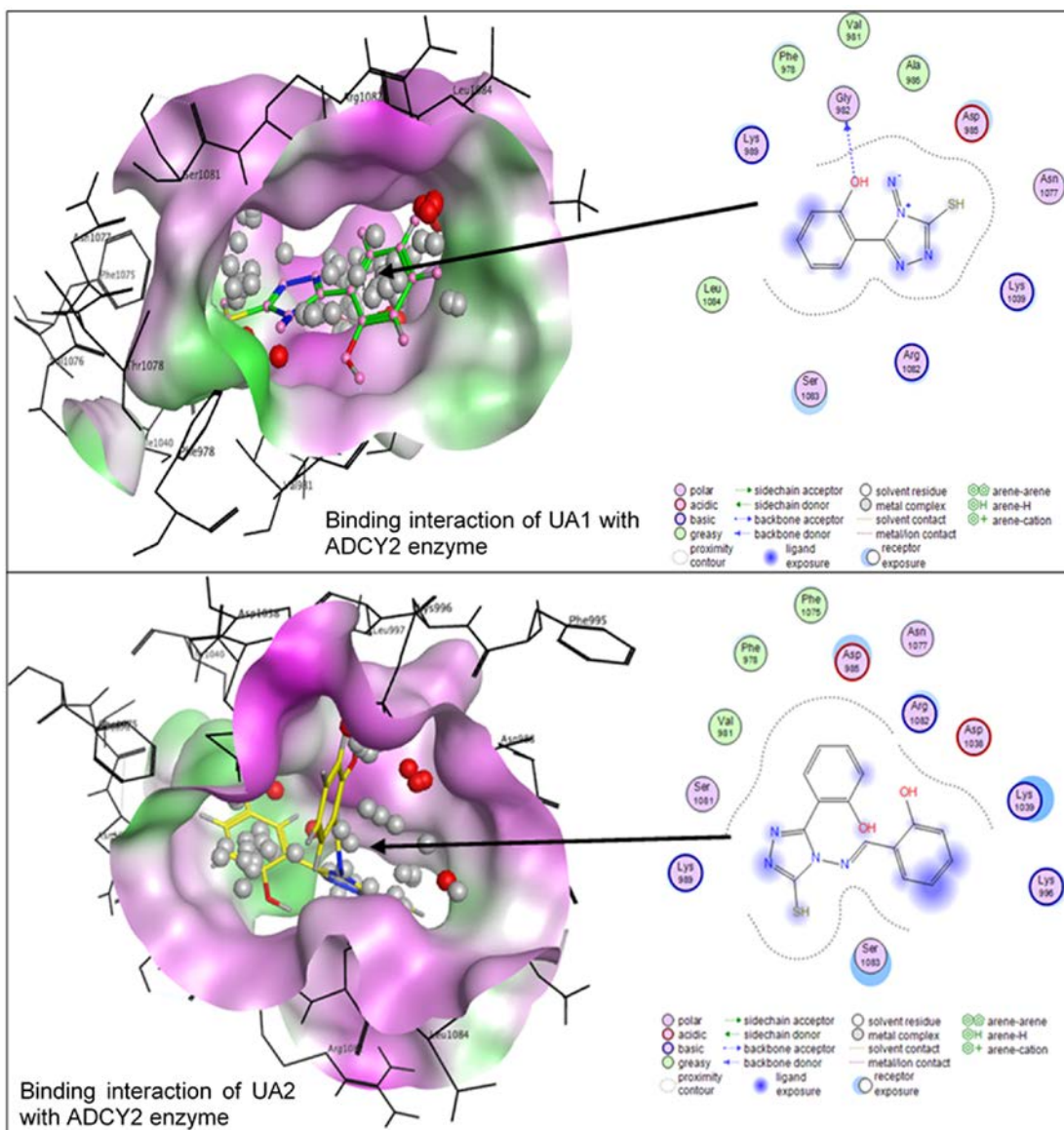


Figure 4: Molecular docking and binding interaction of UA1 and UA2 with the target protein.

Table 1: Characteristic Data of Triazole Molecules.

Molecules	UA1	UA2
Molecular formula	C ₈ H ₈ N ₄ OS	C ₁₅ H ₁₂ N ₄ O ₂ S
Color	Yellow	Yellow
Solubility in water	Not soluble	Not soluble
Solubility in ethanol	Not soluble	Not soluble
melting point	120°C	170°C
Form	Crystalline	Crystalline
R _f value	0.16	0.2

© GSJ

Table 2: FTIR Spectral Analysis for Amino-Triazole Derivatives

Molecules	FTIR (cm-1)
UA1 [4-Amino-5-(2-hydroxyphenyl)-1, 2,4-triazol-3-thione]	3137 cm ⁻¹ stretching (O- H), 2950–3000 (N-H), 1591–1599 stretching (N=C), 1820–1760 (C= O, N-H), 1562–1598 cm ⁻¹ (-C=N), 1313–1365 cm ⁻¹ (-C-N), 1257 (C=C), stretching (-C- O-)
UA2 [4-(2-Hydroxybenzalidine) amine-5-(2-hydroxy) phenyl-1,2,4-triazole-3- thiol]	3061–3100 cm ⁻¹ stretching (O-H), 2950–3000 (N-H), 1591–1599 stretching (N=C), 1760 (C=O), 1562–1598 cm ⁻¹ (-C=N), 1313–1365 cm ⁻¹ (-C-N), 1257 (C=C), stretching (-C-O-)



Table 3: Energy Values Obtained During Docking Analysis of UA1 and Target Protein Adcy2.

S. NO.	MOL	RSEQ	MSEQ	S	RMSD_REFINE	E_CONF	E_PLACE	E_SCORE1	E_REFINE	E_SCORE2
1	UA1	1	1	-4.4328	1.6883	-19.5045	-57.6372	-8.65	-13.7489	-4.4328
2	UA1	1	1	-4.1425	3.179	-20.3494	-55.7177	-8.7457	-13.6448	-4.1425
3	UA1	1	1	-4.0777	4.3644	-16.9346	-68.9705	-8.6376	-14.452	-4.0777
4	UA1	1	1	-4.0583	2.2313	-162.917	-66.9044	-9.0125	-12.7144	-4.0583
5	UA1	1	1	-3.938	2.1873	-19.9674	-55.4801	-9.0106	-10.4294	-3.938
6	UA1	1	1	-3.575	2.3434	-18.4323	-58.6611	-8.887	-6.9816	-3.575
7	UA1	1	1	-3.2458	3.3934	-17.4727	-58.1451	-8.5958	-4.4361	-3.2458



Table 4: Energy Values Obtained During Docking Analysis of UA2 and Target Protein Adcy2.

S. No.	MOL	RSEQ	MSEQ	S	RMSD_REFINE	E_CONF	E_PLACE	E_SCORE1	E_REFINE	E_SCORE2
1	UA2	1	1	-5.2686	1.5623	75.5717	-72.9299	-12.5211	-18.4309	-5.2686
2	UA2	1	1	-5.2331	2.9356	75.0873	-66.3743	-11.1746	-14.9212	-5.2331
3	UA2	1	1	-5.1066	1.4808	75.7112	-72.0299	-11.6525	-17.944	-5.1066
4	UA2	1	1	-5.0353	1.7335	77.7083	-66.87	-11.6234	-16.2194	-5.0353
5	UA2	1	1	-4.8253	2.0812	78.863	-67.3941	-10.9886	-17.6672	-4.8253
6	UA2	1	1	-4.7986	0.6334	77.0574	-91.1087	-11.0898	-10.3277	-4.7986
7	UA2	1	1	-4.6374	1.6071	84.0031	-96.1255	-11.9535	-11.0818	-4.6374
8	UA2	1	1	-4.571	1.9367	79.4771	-68.6839	-10.8255	-15.5981	-4.571
9	UA2	1	1	-4.3266	2.132	77.5481	-84.8722	-11.3369	-4.0335	-4.3266